

This discussion paper is/has been under review for the journal The Cryosphere (TC).  
Please refer to the corresponding final paper in TC if available.

# A statistical approach to refining snow water equivalent climatologies in Alpine terrain

S. Jörg-Hess<sup>1</sup>, F. Fundel<sup>1,\*</sup>, T. Jonas<sup>2</sup>, and M. Zappa<sup>1</sup>

<sup>1</sup>Swiss Federal Institute for Forest, Snow and Landscape Research (WSL), Zürcherstr. 111, CH-8903 Birmensdorf, Switzerland

<sup>2</sup>WSL Institute for Snow and Avalanche Research SLF, Flüelastr. 11, 7260 Davos, Switzerland  
\* now at: German Weather Service, Head Quarters, Offenbach a.M., Germany

Received: 13 June 2013 – Accepted: 12 August 2013 – Published: 26 August 2013

Correspondence to: S. Jörg-Hess (stefanie.joerg@wsl.ch)

Published by Copernicus Publications on behalf of the European Geosciences Union.

Title Page

Abstract

Introduction

Conclusions

References

Tables

Figures

⏪

⏩

◀

▶

Back

Close

Full Screen / Esc

Printer-friendly Version

Interactive Discussion



## Abstract

Gridded snow water equivalent (SWE) are valuable to estimate the snow water resources and verify hydrological models and other models that consider snow as a component of the natural system. However, changing data availability represents a considerable challenge when trying to derive consistent time series for SWE products. In an attempt to improve the product consistency, we first evaluated the differences between two climatologies of SWE grids that were calculated on the basis of data from 110 and 203 stations, respectively. The “shorter” climatology (2001–2009) was produced using 203 stations (*map203*) and the “longer” one (1971–2009) 110 stations (*map110*). Relative to *map203*, *map110* underestimated SWE, especially at higher elevations and at the end of the winter season. We tested the potential of quantile mapping to compensate for mapping errors in *map110* relative to *map203*. During a nine-year calibration period from 2001–2009, for which both *map203* and *map110* were available, the method could successfully refine the spatial and temporal SWE representation in *map110* by making seasonal, regional and altitude-related distinctions. Expanding the calibration to the full 39 yr showed that the general underestimation of *map110* could be removed for the whole winter. The calibrated SWE maps were accurate when averaged over regions and time periods, where the mean error is approximately zero. However, deviations were observed at single grid cells and years. When we looked at three different regions in more detail, we found that the calibration had the largest effect in the region with the highest proportion of catchment areas above 2000 m a.s.l. and that the general underestimation of *map110* could be removed for the entire snow season. The added value of the calibrated SWE climatology is illustrated with practical examples: the verification of a hydrological model, the estimation of snow resource anomalies and the predictability of runoff through SWE.

## Refining SWE climatologies in Alpine terrain

S. Jörg-Hess et al.

Title Page

Abstract

Introduction

Conclusions

References

Tables

Figures



Back

Close

Full Screen / Esc

Printer-friendly Version

Interactive Discussion



## 1 Introduction

Snow plays a crucial role in the hydrological cycle of mountainous catchments (FOEN, 2010; Thayyen and Gergan, 2010; Barnett et al., 2005; Schär et al., 2004). During winter and at high elevations, snow is a temporary buffer for precipitation (Foppa and Seiz, 2012; Foppa et al., 2005; Viviroli et al., 2003). It reduces runoff during winter, but contributes to the total runoff during spring snow melt. In Switzerland, for example, snow is especially relevant as 30 % of the country's annual precipitation falls as snow (Sevruk, 1986), and snowmelt contributes to about 40 % of the total annual runoff (Bernhard and Zappa, 2012). This is why finding a good way to represent the state of snow storage is so relevant for hydrological modelling.

Anomalies in the available snow water resources can impact the hydrological properties of a catchment even several months after the snowfall. Significant changes in runoff during spring and summer may be due to anomalies in the winter snow cover (Cayan et al., 1993). Including an accurate specification of the snowpack for the months preceding model initialisation in long-range model forecasts have been shown to improve the forecast (Day, 1985; Laternser and Schneebeli, 2003; Clark and Hay, 2004; Schär et al., 2004; Hock et al., 2006; Bierkens and van Beek, 2009; Pagano et al., 2009; Koster et al., 2010).

Long series of high quality snow storage data (snow climatologies) are desirable for many applications. Some examples include the risk assessment of droughts and floods, e.g., to estimate the return periods of critical events (Beniston, 2012); the classification of winters according to their snow availability; the parameter calibration of hydrological models (Parajka and Blöschl, 2008); the validation of snow cover simulations from regional climate models (Steger et al., 2012) and land-surface models (Dutra et al., 2011); the study of changes in the water balance of large-scale basins such as the Rhine river, where snow significantly contributes to the total runoff (Mauser et al., 2007; Poulin et al., 2011).

### Refining SWE climatologies in Alpine terrain

S. Jörg-Hess et al.

Title Page

Abstract

Introduction

Conclusions

References

Tables

Figures



Back

Close

Full Screen / Esc

Printer-friendly Version

Interactive Discussion



## Refining SWE climatologies in Alpine terrain

S. Jörg-Hess et al.

[Title Page](#)[Abstract](#)[Introduction](#)[Conclusions](#)[References](#)[Tables](#)[Figures](#)[◀](#)[▶](#)[◀](#)[▶](#)[Back](#)[Close](#)[Full Screen / Esc](#)[Printer-friendly Version](#)[Interactive Discussion](#)

Snow information is usually obtained for hydrological models via remotely sensed snow cover products or in-situ observations (Andreadis and Lettenmaier, 2005; Clark et al., 2006; Slater and Clark, 2006). To provide accurate snow storage information for catchments and larger regions, spatially distributed snow water equivalent (SWE) information is desirable.

Estimating the spatial snow depth distribution in Switzerland has been the focus of several studies. Witmer et al. (1986) considered the regional and topographical dependencies in seven climatological regions in Switzerland to calculate gridded maps of climatological monthly snow depths (mean, median and 80 percentile) based on data from 160 snow stations. They found that the linear dependency of snow depth and elevation cannot account for the local variability in the snow depth. In a different approach Auer et al. (2004) describe the correlation between snow depth and altitude using an area-wide base value. This value is adjusted with a compensation value based on the regional residuals between the base value and the measured values. At the Swiss Federal Institute for Snow and Avalanche Research, Davos (SLF), such a snow depth map is produced on a weekly basis during the winter months. The spatial patterns of the snow depth calculated with this model agree well with the precipitation maps of the Alps contained in FOEN (2010), which are based on a different approach. Generating gridded snow maps typically involves tackling various obstacles. The correct placing of the seasonal snow line is challenging if the estimation is based on station measurements. Another difficulty is that snow observations at lower altitudes are often not conducted in early winter and spring. Snow information from real-time snow cover maps based on satellite data can significantly improve the gridded snow information, and have thus been integrated into SLF's operational production of snow depth maps (Foppa et al., 2005, 2007).

In Switzerland daily snow depth readings are recorded at hundreds of stations, but SWE measurements are rarely made and only about 40 locations provide bi-weekly data. However, with snow density models (e.g., Jonas et al., 2009; Sturm et al., 2010) it is possible to convert operational snow depth maps into SWE maps.

## Refining SWE climatologies in Alpine terrain

S. Jörg-Hess et al.

Title Page

Abstract

Introduction

Conclusions

References

Tables

Figures

◀

▶

◀

▶

Back

Close

Full Screen / Esc

Printer-friendly Version

Interactive Discussion



A similar concept is used in this study to produce base climatologies in the form of daily SWE maps (see Sect. 3.1). However, varying station densities over the past decades mean that the mapping accuracies also vary greatly over time. To investigate and mitigate this problem, two climatologies with daily SWE maps were analysed: a long-term data set (39 yr, 1971–2009) based on a small number (110) of stations, i.e. a sparse network, and a short-term data set (9 yr, 2001–2009) based on considerably more stations (203), i.e. a dense network. Data from sites above 2000 m a.s.l. are only contained in the second data set. As about 23 % of Switzerland is above 2000 m a.s.l., accurate information about the snow mass at higher altitudes is crucial.

The aim of this study was to identify a calibration methodology that can refine the gridded SWE maps based on the sparse station network, so that they can be homogenized with the maps based on the dense station network. The statistical calibration method “quantile mapping” is applied, where a quantile according to the non-exceedance probability in the “sparse” climatology is modified to meet the quantile of the same non-exceedance probability in the “dense” climatology (Panofsky and Brier, 1968). The quality of the calibrated SWE maps is evaluated and their added value for selected practical applications is tested. Possible applications of the data set are demonstrated with three examples: (1) SWE climatologies are compared with SWE estimated with a hydrological model; (2) snow resource anomalies are estimated based on the SWE climatologies; and (3) predicting low flow at the main river gauge of the Alpine Rhine catchment in Neuhausen is evaluated.

## 2 Study regions and data

### 2.1 Test catchments

Gridded SWE maps were created, calibrated and evaluated for the whole of Switzerland. A detailed evaluation is presented here for three sub-areas, namely the Alpine

## Refining SWE climatologies in Alpine terrain

S. Jörg-Hess et al.

Title Page

Abstract

Introduction

Conclusions

References

Tables

Figures

◀

▶

◀

▶

Back

Close

Full Screen / Esc

Printer-friendly Version

Interactive Discussion



Rhine (AR), Valais (VS) and the region including the rivers Thur, Toess and Glatt (TGG) (Fig. 1). The regions were selected to take into account different elevation ranges and assess the importance of snow as a controlling element of the runoff regime. The main characteristics of the three regions are given in Table 1. AR and VS are alpine catchments where the seasonal shape of runoff generation is strongly influenced by snow and glacier melting with a distinct summer maximum. The annual mean runoff is 1200 mm in AR and 1100 mm in VS. The highest runoff is observed during spring in the TGG catchment, with an annual mean runoff of 850 mm. Precipitation is high in TGG ( $1400 \text{ mm yr}^{-1}$ ) and AR ( $1300 \text{ mm yr}^{-1}$ ), and slightly lower in VS ( $1000 \text{ mm yr}^{-1}$ ). The annual average temperature is affected by the altitudes of the catchment. It is rather low in VS ( $1.8^\circ\text{C}$ ) and AR ( $3.1^\circ\text{C}$ ), and higher in TGG ( $8.1^\circ\text{C}$ ). Temperature and precipitation are taken from the meteorological forcing used by Zappa et al. (2012) for a hydrological simulation for all of Switzerland.

## 2.2 Snow observations

A common measure in monitoring snow resources is the height of the snow cover (HS). To estimate the available water resources in specific areas, however, the snow water equivalent (SWE) is a more relevant variable as it represents the water content of snow. In Switzerland, more HS measurements are available than SWE measurements simply due to the fact that measuring HS requires less effort than measuring SWE. However, HS and SWE are strongly correlated with each other (Sturm et al., 2010).

The gridded SWE maps used in this study were derived from HS measurements from several station networks. Automated measurements are available from the ANETZ (Automatisches MessNETZ) and ENET (ErgänzungsNETZ) network of the Federal Office of Meteorology and Climatology MeteoSwiss and from IMIS (Interkantonales Mess- und Informationssystem), run by SLF. Moreover, the SLF observers for the avalanche forecast service record manual HS readings daily.

Over the past decades the number and extent of measurement sites in Switzerland has increased steadily. The IMIS network was founded in the late 1990s and extended

the existing networks to elevations above 2000 m.a.s.l. For the creation of the gridded SWE maps, stations were selected according to data availability and representativeness. Two sets of HS measurements, based on a different number of stations and spanning different periods were built for the calibration (Fig. 1): 110 stations from 1971 to 2009 (d110; purple dots) and 203 stations from 2001 to 2009 (d203; purple, orange and green dots). A third data set, based on 133 stations from 1989 to 2009 (d133; purple and orange dots), was used to select 23 independent stations to validate the calibration procedure before 2001. The measurement accuracy depends on the equipment and accounts for about  $\pm 2$  cm.

Based on d110 and d203 daily, gridded SWE maps, *map110* and *map203*, were produced for Switzerland with the model described in Sect. 3.1. *Map133* is the gridded SWE climatology based on d133.

## 2.3 Runoff observations

For the application example in Sect. 5.1, daily runoff records from the river gauge in Neuhausen (yellow triangle in Fig. 1), operated by the Swiss Federal Office for the Environment, were used. The river gauge Neuhausen is located downstream of Lake Constance ( $> 500$  km<sup>2</sup>), at an altitude of 383 m.a.s.l., with a drainage area of 11 887 km<sup>2</sup>. This station on the river Rhine is particularly interesting as Lake Constance decreases the anthropogenic runoff fluctuations. The catchment of the Alpine Rhine is affected by lake regulation, river corrections and hydropower.

## 3 Methods

### 3.1 Snow water equivalent mapping

Maps of SWE are produced using a two-step procedure. The available HS station data is first converted to SWE, and then mapped onto grid using a snow-specific detrended distance weighting approach. To calculate SWE from the observed HS, an estimation

Title Page

Abstract

Introduction

Conclusions

References

Tables

Figures



Back

Close

Full Screen / Esc

Printer-friendly Version

Interactive Discussion



of the snow bulk density  $\rho b$  is required:

$$\text{SWE} = \rho b \cdot \text{HS}. \quad (1)$$

Snow bulk density can be predicted from the HS, day of the year, altitude and snow region in Switzerland using a parametric model (Jonas et al., 2009). The model was calibrated on a data set of 11 000 SWE-HS measurements from 48 winters (1960–2008) and 37 stations throughout the Swiss Alps, and is thus particularly suitable for this study. We used an enhanced version of the model to mitigate a problem noticeable when the model is applied to convert a time series of daily data, as noted in Jonas et al. (2009). Contrary to the original version of the model, the enhanced version is now capable of distinguishing snowpack settling from snow melt by assimilating daily HS data instead of a singular HS reading only.

Daily SWE data estimated for each of the stations used for the climatologies were mapped onto a digital elevation model (DEM) with a horizontal resolution of 1 km. A non-linear trend of SWE over elevation was first calculated for each day using median values calculated for overlapping elevation windows. Detrended SWE values, i.e. the offset of each reading from the trend, are then interpolated to the grid using a distance-weighting approach based on a Gaussian filter for each grid cell  $i$ . As the SWE distribution is strongly correlated with elevation, we used a linear combination of two separate Gaussian filters, one for horizontal distances ( $\text{distance}_h$ ) and one for vertical distances ( $\text{distance}_v$ ).

$$\text{Weight}_i = \exp \left( -0.5 \cdot \left( \frac{\text{distance}_h}{\text{filter width}_h} + \frac{\text{distance}_v}{\text{filter width}_v} \right)^2 \right) \quad (2)$$

Optimized filter widths for snow mapping in Switzerland are roughly around 25 km horizontally and 500 m vertically, depending on the station density and season. Finally, the detrended and mapped SWE data was reprojected onto the DEM.

The above procedure was applied to calculate the three SWE climatologies outlined in Sect. 2.2. The longest climatology based on 110 stations only allowed for a detrend-

ing up to 2100 m.a.s.l. Above this elevation, the SWE maps will probably underestimate the true SWE. In contrast, the shortest climatology based on 203 stations allowed for a detrending up to 2700 m.a.s.l. Moreover, the increased number of stations enabled a regional detrending using only the nearest 40 stations around each location, resulting in an enhanced resolution of regional patterns.

### 3.2 Quantile mapping

Quantile mapping was used to calibrate *map110* based on *map203* (Panofsky and Brier, 1968) and applied for the daily precipitation and temperature corrections (Ines and Hansen, 2006; Fundel et al., 2010; Bardossy and Pegram, 2011; Themeßl et al., 2011; Thrasher et al., 2012), the calibration of climate scenarios (Li et al., 2010; Veijalainen et al., 2012) and hydrological applications (Wood et al., 2004; Boe et al., 2007). In this study the empirical cumulative distribution function (ECDF) was used. It makes the application very flexible as no assumptions about the distribution are needed (Themeßl et al., 2011).

The exceedance probability of an SWE value in *map110* was assumed to correspond to the quantile of the same exceedance probability in *map203* (Fig. 2). The ECDFs are  $F^l$  for *map110* and  $F^h$  for *map203* in the overlapping period. The calibrated SWE was then obtained by:

$$\text{SWE}_{\text{cal}} = F^{h-1}(F^l(\text{SWE}_i)) \quad (3)$$

The data used was stratified according to altitude, region and amount of snow to address different error characteristics as described in Sect. 4.2. The main advantages of quantile mapping are its simplicity and the applicability to all variables, independent of the underlying distribution. A disadvantage is the handling of “new extremes”, which exceed the values within the training period. Extremes larger than those observed could be dealt with by e.g.: performing a double quantile-quantile transformation (Bardossy and Pegram, 2011), extrapolating to values exceeding the observations (Boe et al., 2007), combining extreme value analysis and non-parametric regression methods to fit

## Refining SWE climatologies in Alpine terrain

S. Jörg-Hess et al.

Title Page

Abstract

Introduction

Conclusions

References

Tables

Figures

◀

▶

◀

▶

Back

Close

Full Screen / Esc

Printer-friendly Version

Interactive Discussion



the tails of the distributions (Bogner et al., 2012) and applying a transfer function based on model output and observations to future or past observations (Li et al., 2010). In this study, values of the calibration period exceeding the largest value of the training period are set equal to the largest value of the training period.

Another drawback of quantile mapping is that for individual cases a correction may go in the wrong direction (Hamill and Whitaker, 2006). Quantile mapping corrects the shape of the distribution function and can therefore also reduce errors in variability (Themeßl et al., 2011). While bias and variability can be reduced with quantile mapping, errors in the higher-order moments can probably not to be removed.

### 3.3 Validation methods

The gridded SWE maps are validated taking into consideration the mean error (ME), the squared correlation coefficient ( $R^2$ ) and the root mean squared error (RMSE). In order to ensure that small fluctuations in SWE are preserved,  $R^2$  is calculated with the seasonal trend removed. Therefore the first-order differences with a lag of one year are used (Wilks, 2006; Foppa et al., 2007; Saloranta, 2012).

## 4 Results

In this study, *map203* is assumed to contain more accurate gridded snow information and is therefore considered as the reference data set.

### 4.1 Quality of the SWE maps

The spatial variability of the snow cover led to uncertainty in the error statistics, which are based on station data. To put this into perspective, consider the following illustration: If the whole modelling domain was covered by 2 m of snow, but with a realistic small-scale variability of  $\pm 15\%$  (Jonas et al., 2009), a perfect coarser-scale SWE product would arrive at a homogeneous distribution of 2 m. However, given that station data

Title Page

Abstract

Introduction

Conclusions

References

Tables

Figures

◀

▶

◀

▶

Back

Close

Full Screen / Esc

Printer-friendly Version

Interactive Discussion



represent single point measurements with natural deviations from the mean, the resulting RMSE would amount to 330 mm, even though the mapping model is otherwise perfect.

The impact of each individual station on the mapping results and its regional representativeness were investigated with a “leave one out cross-validation” approach (LOO-CV). At each measurement station, SWE was estimated first with the associated station ( $SWE_{orig}$ ) and then without ( $SWE_{loo-cv}$ ). The altitude was adjusted to the station altitude by subtracting the day-specific SWE gradient from the modelled SWE values. “Orig” and “loo-cv” were compared to identify the uncertainty of the model and the impact of individual stations on the mapping results.

Averaged over all stations,  $SWE_{orig}$  outperforms  $SWE_{loo-cv}$  (Fig. 3). It should be considered that a representative value for the region ( $1 \times 1$  grid) was compared to a single measurement that is unlikely to represent the spatial distribution of snow depth (Bloschl, 1999). However, the small differences between “orig” and “loo-cv” indicate that the uncertainty between the stations is only slightly larger than at the station locations. From December to April, the uncertainty increases at many stations (not shown) because the melting process causes large SWE differences between high and low altitudes. RMSE increases with altitude due to the higher proportion of snow with respect to total precipitation. The small RMSEs at lower elevations, where SWE is generally small, do not necessarily indicate better performance of the estimations for these regions.  $R^2$  is generally very high and seems to be independent of elevation and the related snow amount. In regions with a higher station density,  $R^2$  is higher. The lowest  $R^2$  values are observed in regions (and months) where the ablation and accumulation of snow are difficult to separate clearly.

## 4.2 Differences between SWE climatologies

To reveal systematic errors and to find a meaningful way to stratify the data for the calibration procedure, the difference between *map110* and *map203* ( $\Delta SWE = map110 - map203$ ) was analysed for all of Switzerland during the overlap-

## Refining SWE climatologies in Alpine terrain

S. Jörg-Hess et al.

Title Page

Abstract

Introduction

Conclusions

References

Tables

Figures

◀

▶

◀

▶

Back

Close

Full Screen / Esc

Printer-friendly Version

Interactive Discussion



ping period (2001–2009). The  $RMSE_{orig}$  for the 110 stations appearing in both data sets is slightly smaller for *map203* (34 mm) than for *map110* (36 mm). Different aspects such as altitude, snow depth, seasonality and regionally specific characteristics were analysed.

5 Compared to *map203*, *map110* underestimates SWE, especially at high elevations (Fig. 4). At lower altitudes however, the differences are negligible. This finding comes as no surprise since the 110 available stations for *map110* only allowed for a detrending up to 2100 m a.s.l., but stations from *map203* also cover altitudes above 2100 m a.s.l. It is therefore of no advantage to use e.g. grid cells at an altitude of 2000 m a.s.l. to  
10 to calibrate a grid cell at 1000 m a.s.l. The error characteristics depend on altitude and thus a classification into elevation ranges is justified. The mean  $\Delta SWE$  is independent of snow amount (Fig. 4). It is close to zero for both snow-rich and snow-poor days, but the variance is higher for snow-rich days. The distinction between snow-rich days (SR, SWE exceeds the average) and snow-poor days (SP, SWE smaller than the av-  
15 erage) is based on the median in *map110*. The same days are considered as having correspondingly rich or poor snow resources in *map203*.

$\Delta SWE$  varies spatially between the regions and altitudes, and temporally between December, January, February, March and April (Fig. 5). From December to April, the  $\Delta SWE$  for a large area increases. The SWE height trend has a small gradient in De-  
20 cember. Therefore, the benefits of having stations at higher elevations are smaller in December than at the end of the winter season. This is confirmed by the fact that the differences in December are small and those in April are much higher. The highest underestimations of *map110* are observed in the VS and part of the AR catchment. Overestimations are observed only in the eastern part of VS (Gotthard region). The  
25 region with the largest differences is similar to the region above 2000 m a.s.l. (area shaded in grey in Fig. 1).

## Refining SWE climatologies in Alpine terrain

S. Jörg-Hess et al.

[Title Page](#)[Abstract](#)[Introduction](#)[Conclusions](#)[References](#)[Tables](#)[Figures](#)[⏪](#)[⏩](#)[◀](#)[▶](#)[Back](#)[Close](#)[Full Screen / Esc](#)[Printer-friendly Version](#)[Interactive Discussion](#)

### 4.3 Implementing the quantile mapping

The outcome of the comparison in the previous section led to the definition of the calibration procedure illustrated in Fig. 6. Starting with *map110* and *map203*, the calibration of *map110* is implemented separately for each grid cell to account for spatial and altitude-dependent differences, and for each day with a moving window of  $\pm 15$  days to account for seasonal effects. For dates before 15 December and after 15 April reduced classes were used as the maps are available only from 1 December till 30 April. Additionally snow-rich (SR) and snow-poor (SP) days were distinguished by means of the median SWE in *map110*. This procedure results in a calibrated data set of gridded SWE maps for 39 yr (*map.ca*).

#### 4.3.1 Application during the overlapping period

The calibration was first tested for the 9 overlapping years (2001–2009) and the relation obtained between the quantiles of the two data sets was then applied to the 39 available years (1971–2009) of *map110*. The nine overlapping years were cross-calibrated. By dividing the data set into a training period (eight years) and a calibration period (one independent year), each year can be calibrated independently with the remaining eight years. For instance, for a specific grid cell “x” (star in Fig. 1), the calibration for 11 March 2003 uses all days of this grid cell from 24 February to 26 March except those from the year 2003 to produce  $F_{11 \text{ Mar, x}}^h$  and  $F_{11 \text{ Mar, x}}^l$ . The median of  $F_{11 \text{ Mar, x}}^l$  is 493 mm, which we now define as the threshold to discriminate snow-rich from snow-poor days. The same days are also considered as snow-rich and snow-poor in *map203*. On this day a SWE of 539 mm is altered to 588 mm by using only the snow-rich days from *map110* and the same days from *map203* for the calibration.

TCD

7, 4241–4286, 2013

## Refining SWE climatologies in Alpine terrain

S. Jörg-Hess et al.

Title Page

Abstract

Introduction

Conclusions

References

Tables

Figures

◀

▶

◀

▶

Back

Close

Full Screen / Esc

Printer-friendly Version

Interactive Discussion



### 4.3.2 Application before the overlapping period

For the entire period (39 yr), quantile mapping is, as before, completed for each grid cell and day separately by distinguishing snow-rich and snow-poor days based on the median of *map110* during the overlapping period. The reallocation of SWE values follows a simple procedure, which is illustrated here for the grid cell “x” on 16 January 1979.  $F_{16 \text{ Jan, x}}^h$  and  $F_{16 \text{ Jan, x}}^l$  contain all January days of grid cell “x” from 2001–2009 and 1971–2009, respectively. The threshold to separate snow-rich and snow-poor days is chosen during the overlapping period to ensure that both data sets are separated on the basis of the same conditions. For grid cell “x”, the median SWE on 16 January is 285 mm from 2001–2009 and 297 mm from 1971–2009. For this grid cell the difference is small. The threshold of 285 mm classifies the SWE of 299 mm on 16 January 1979 as snow-rich. Thus  $F_{16 \text{ Jan, x}}^l$  and  $F_{16 \text{ Jan, x}}^h$  use only snow-rich days to calibrate the SWE of 16 January 1979 to a refined value of 302 mm.

### 4.4 Validation of the quantile mapping

The calibrated SWE maps were first validated with *map203*. As a simple cross-validation for every station is very time consuming, we opted for two different approaches in order to validate our maps during both the calibration period (CP, 2001–2009) and the test period (TP, 1989–2000).

#### 4.4.1 Cross-calibration

In order to validate the cross-calibration during the calibration period (CP, 2001–2009), *map203* was considered as reference. The ME,  $R^2$  and RMSE were calculated for each grid cell separately and averaged over the regions AR, TTG and VS (Table 2). The performance of the SWE simulation differs between *map110* and *map.cal*, as well as between the regions. *Map.cal* outperforms the uncalibrated *map110* in all regions. As expected, after calibration the ME is negligible and RMSE is smaller.  $R^2$  of the trend-

## Refining SWE climatologies in Alpine terrain

S. Jörg-Hess et al.

[Title Page](#)[Abstract](#)[Introduction](#)[Conclusions](#)[References](#)[Tables](#)[Figures](#)[◀](#)[▶](#)[◀](#)[▶](#)[Back](#)[Close](#)[Full Screen / Esc](#)[Printer-friendly Version](#)[Interactive Discussion](#)

## Refining SWE climatologies in Alpine terrain

S. Jörg-Hess et al.

Title Page

Abstract

Introduction

Conclusions

References

Tables

Figures

◀

▶

◀

▶

Back

Close

Full Screen / Esc

Printer-friendly Version

Interactive Discussion



corrected SWE grid cell by grid cell is relatively high, with values above 0.7. Thus small fluctuations in the snow depth are still reproduced after calibration. At regions above 2000 m.a.s.l.  $R^2$  is higher after calibration. Otherwise, however it is generally smaller, because some values in *map110* are shifted to the maximum or minimum in *map203*, while the SWE in *map203* remains variable. As quantile mapping can sometimes correct in the wrong direction, a reduction in the bias is at the expense of the  $R^2$ . Even though the performance is good after calibration, the regional differences, especially in  $R^2$  and RMSE persist. Some of these differences are related to differences in the altitude ranges and station densities in the three regions investigated.

The daily regional SWE of *map.cal* accord good with those of *map203* (Fig. 7). Until March *map110* agrees quite well with *map203*. The divergence increases towards the end of April. These underestimations of *map110* compared to *map203* could be removed with calibration (*map.cal*) over the entire winter in all three catchments. As in the TTG region no additional stations are available, the differences between *map110* and *map203* in the TTG catchment are caused by the regional detrending applied to *map203* and the detrending reaching up to 2700 m.a.s.l. Systematic over- or underestimations in  $\Delta$ SWE, which differ between months and grid cells (upper row of Fig. 8), could be generally removed through the calibration (lower row of Fig. 8). The interquartile range (IQR) of the differences between  $\Delta$ SWE and *map.cal*–*map203* is unchanged (not shown). Generally, the correction value is more pronounced at high quantiles (Fig. 9). The lowest 30 percentiles of *map110* agree well with *map203*. The calibration is effective for the remaining two-thirds of all values. However the 100 percentile is changed to the maximum of *map110* in the CP. This is clearly a limitation when adopting quantile mapping. We will elaborate on this later.

### 4.4.2 Spatial and temporal consistence

For the spatial evaluation, *map203* was “re-modelled” during the CP by removing four stations in the subareas VS and AR (*map203<sup>-</sup>*). The stations removed are: Obersaxen (OB, 1420 m.a.s.l.), Parsenn Kreuzweg (PA, 2290 m.a.s.l.), Anniviers Orzival (AN,

2630 m.a.s.l.) and Binn (BI, 1410 m.a.s.l.). They are labelled and marked with a black outline in Fig. 1. Thus in both regions a station above 2000 m a.s.l. and a station at about 1500 m a.s.l. were removed. The resulting calibrated SWE maps are denoted *map.cal*<sup>-</sup>. Generally the interpolation performed without the four selected stations (*map203*<sup>-</sup>) results in a higher RMSE (Table 3). In VS (AN and BN), the RMSE is larger than in AR (OB and PA). The relative effect of removing stations is, however, greater in the AR region. For the calibrated maps, the RMSE is only slightly smaller in *map.cal* than in *map.cal*<sup>-</sup>, except for BN. The omission of the selected stations has only a small influence on the uncertainty of the calibrated maps at the station locations. Thus we conclude that the calibration works equally well at grid cells with observations as in between such grid cells.

The temporal validation outside the calibration period is done by comparing the test period (TP) and the calibration period (CP). The calibrated maps are compared with measurements of the 23 “independent” stations from *map133* (Fig. 1). The median of the differences is similar during CP (-1.3) and TP (-2.1) (Fig. 10), but the interquartile range and total variance are slightly larger during TP. The mean differences vary between the stations. However, the mean and variance of the differences at most stations are similar between CP and TP. This similarity indicates that the calibration procedure is temporally consistent.

## 4.5 Trend

SWE anomalies of *map110* are maintained in the maps calibrated with *map203* (Fig. 11). The linear regression for mean winter SWE resulted in insignificant regression coefficients. However, the coefficients and *p* values of the linear regression from *map110* and *map.cal* are very similar. Therefore SWE anomalies from the median winter SWE were compared for different altitude ranges. The correlation coefficients of *map110* and *map.cal* are typically very high (> 0.85). Based on the station background anomalies of median winter SWE are expected to be similar up to 2000 m.a.s.l. We expected however that there are SWE anomalies that are only present at higher altitudes

Title Page

Abstract

Introduction

Conclusions

References

Tables

Figures



Back

Close

Full Screen / Esc

Printer-friendly Version

Interactive Discussion





the gridded SWE maps (blue, red and green) are only supplied from 1 December until 31 April. The seasonal evolution of SWE is similar between the versions of the same year and region. The validation of the PREVAH simulation yields different conclusions depending on which gridded SWE map is taken as a reference. In the year 2007/08, *map203* is available and is considered the best reference. In this case, the snow resources simulated with PREVAH are generally underestimated in the AR region (ME: -29 mm), and partly over- and underestimated in the VS region (ME: -1 mm). If we take *map110* as the reference, PREVAH only estimates SWE accurately for a few weeks at the end of winter season in the AR region (ME: -19 mm) and overestimates SWE in the VS region (ME: 21 mm). In both cases, the wrong conclusions are drawn when *map110* serves as the reference. As the calibration of *map110* changes the SWE values towards the *map203* estimates, the model verification would be more realistic if *map.cal* instead of *map110* were taken as reference. For the year 1990/1991, for which *map203* is not available, *map.cal* is a very valuable data base for verification, especially at the end of winter season, where the snow resources are underestimated by *map110*. To calibrate and verify hydrological models against SWE for periods covering the calibration period (2001–2009) and the period before, *map.cal* should be used as the reference to ensure a consistent, high quality data set.

## 5.2 Estimation of snow resources anomalies

For research on the water resources in Switzerland or on lake and reservoir management, calculating spatially explicit SWE anomalies is becoming increasingly important, as is comparing current with past situations. Here calibrated long-term SWE climatology is helpful. According to the underlying climatology (*map110* or *map.cal*), various conclusions about the anomalies of a certain winter can be drawn (Fig. 13). The aim is not to decide on how good the two climatologies are. The seasonal pattern and snow amount of the two climatologies agree quite well until March. At the end of the season, the median is lower and the variability is larger in the climatology based on *map110*. Both climatologies yield negative SWE anomalies for the winter 2004/2005 (red line in

## Refining SWE climatologies in Alpine terrain

S. Jörg-Hess et al.

Title Page

Abstract

Introduction

Conclusions

References

Tables

Figures



Back

Close

Full Screen / Esc

Printer-friendly Version

Interactive Discussion



Fig. 13). However, at the end of the winter season in April, if the *map110* climatology is used, the anomaly is still in the interquartile range, whereas in the climatology of *map.cal* the negative anomaly is larger.

### 5.3 Predictability of runoff in Neuhausen with SWE in the Alpine Rhine Catchment

The aim of the third application is to illustrate the value of distributed SWE for estimating low-water events in the following summer using the example of the runoff observed in Neuhausen (yellow triangle in Fig. 1). The minimum daily runoff of each year (1971–2009) was determined for the months of May, June and July. The snow volume used to determine the range of the minimum runoff is the calibrated SWE on 15 April of each year averaged over the catchment of the Alpine Rhine. The scatter plot of 15 April SWE and the minimum runoff in May (left), June (middle) and July (right) are shown in Fig. 14. A linear regression is carried out for the log-transformed variables, SWE and runoff (black curve). The 95 % predictive interval is calculated to specify the range where minimal runoff can be expected (Weisberg, 2005) (dotted lines). The predictive interval is larger than the confidence interval because in addition to the estimates uncertainty, the uncertainty of the predictor is also taken into account.

Generally, the minimum runoff is positively related to 15 April SWE. In May the regression curve is rather flat, whereas the relation is more pronounced in July, and even more in June. The variability increases from May to July due to the smaller base values of the snow melt. We are interested in the lower curve of the prediction interval to predict worse case scenarios. The minimum expected runoff is about 40 % lower if 15 April SWE is 200 mm than if 15 April SWE is 500 mm (Fig. 14). As illustrated here with 15 April SWE in the Alpine Rhine region, this strategy can be used to create look-up tables for different dates in the winter season and select simple early indicators for low flow in alpine rivers. These indicators only contain SWE, and thus display the minimum that must be expected for cold conditions with little precipitation.

## Refining SWE climatologies in Alpine terrain

S. Jörg-Hess et al.

Title Page

Abstract

Introduction

Conclusions

References

Tables

Figures

◀

▶

◀

▶

Back

Close

Full Screen / Esc

Printer-friendly Version

Interactive Discussion





## Refining SWE climatologies in Alpine terrain

S. Jörg-Hess et al.

Title Page

Abstract

Introduction

Conclusions

References

Tables

Figures

◀

▶

◀

▶

Back

Close

Full Screen / Esc

Printer-friendly Version

Interactive Discussion



for single years and grid cells, the method and its underlying assumptions might not be free of errors. Therefore using or evaluating single grid cells is not recommended. The evaluation with independent stations and stations outside the calibration period showed that the calibration still could reduce the uncertainty spatially and temporally compared to *map110*. It is therefore very useful for obtaining information on the water storage in a snowpack on a catchment scale and for investigating SWE anomalies during the recent past.

For the statistical calibration method, quantile mapping, it is important to investigate possible changes in the distribution of SWE during the periods 1971–2000 and 2001–2009. Figure 15 illustrates the CDFs of these two periods. The two distributions can be considered similar, which means it is not necessary to perform a double quantile-quantile transformation or other transfer functions such as those used by Bardossy and Pegram (2011) and Li et al. (2010). The maximum for *map110* (1949 mm), however, is larger than the maximum for *map203* (1353 mm). Although there are several ways to handling such “new” extremes, we decided to change the values of *map110* that exceeded the maximum of *map203* to the maximum of *map203*, as the maximum of the training period is exceeded only in  $6.4 \times 10^{-4}$  % of the sample considered. As we showed in Fig. 11, the anomalies in SWE are preserved in the 39 yr calibration period. This makes us confident that the method, as we applied it, can be used for different periods in the past and the future.

A closer look at Table 2 shows that the calibration could reduce the RMSE in all regions. For the three study regions, we can conclude: in the region of the rivers Thur, Töss and Glatt, the RMSE could be reduced from 14 to 9 mm. The differences between *map203* and *map110* are mainly due to changes in the global height trend calculation, as no additional stations have been established in the catchment since 1971. *Map110* calculates the global height trend for all of Switzerland, whereas in *map203* it is computed separately for seven predefined snow regions. In Valais, the discrepancy between *map203* and *map110* is larger than in the other two study areas. We assume that this is due to it having a large area above 2000 m a.s.l. In *map110* the global snow

depth trend is flat above 2000 m.a.s.l., while this height trend is drawn further up to 2700 m.a.s.l. in *map203*. Here the RMSE is diminished from 78 to 61 mm. The detailed analysis of the Alpine Rhine indicate, that the largest deviations of the two climatologies are at the end of winter and at higher elevations, when the RMSE is reduced from 54 to 48 mm.

From these findings, we can conclude that the general underestimation of *map110* could be removed over the entire snow period. We have seen that the benefit of including additional stations is smaller at the beginning of the snow season in December due to a small height gradient in SWE, which increases toward April, at the end of the snow season. The calibration has therefore little potential at the beginning of snow season to refine SWE values and more potential at the end of the winter season. Because of the large variability of SWE in Switzerland, the calibrated SWE climatology presented, provides probably the best overview of Swiss snow resources for the recent past. The mean difference between *map203* and *map110* could be reduced from  $-18 \text{ mm}$  to  $7 \cdot 10^{-3} \text{ mm}$  after quantile mapping.

The gridded SWE climatologies presented are an important contribution to water resource research and applications. Three possible applications have been discussed. *Map.cal* provides a consistent basis for verifying and parameterising the snow module of fully distributed or semi-distributed hydrological models within the period 1971–2009. The second application showed the importance of a long SWE climatology, approximating current SWE maps, for estimating SWE anomalies. The third application illustrated the potential for forecasting minimum expected runoff in May, June or July using the SWE on 15 April as sole predictor. We found that in the region of the Alpine Rhine snow anomalies correlated with the streamflow anomalies of the following season, as did Cayan et al. (1993).

Research with gridded SWE climatologies will always need an update to take into account the latest developments in snow modelling to ensure that it has the best available data. The SWE maps used in this study exhibit, for example, weaknesses in the correct placement of the snow-no snow borderline and the effect of sub-grid variabil-

## Refining SWE climatologies in Alpine terrain

S. Jörg-Hess et al.

[Title Page](#)[Abstract](#)[Introduction](#)[Conclusions](#)[References](#)[Tables](#)[Figures](#)[◀](#)[▶](#)[◀](#)[▶](#)[Back](#)[Close](#)[Full Screen / Esc](#)[Printer-friendly Version](#)[Interactive Discussion](#)



## Refining SWE climatologies in Alpine terrain

S. Jörg-Hess et al.

Title Page

Abstract

Introduction

Conclusions

References

Tables

Figures

◀

▶

◀

▶

Back

Close

Full Screen / Esc

Printer-friendly Version

Interactive Discussion



Bierkens, M. F. P. and van Beek, L. P. H.: Seasonal predictability of European discharge: NAO and hydrological response time, *J. Hydrometeorol.*, 10, 953–968, doi:10.1175/2009jhm1034.1, 2009. 4243

Bloschl, G.: Scaling issues in snow hydrology, *Hydrol. Process.*, 13, 2149–2175, doi:10.1002/(sici)1099-1085(199910)13:14/15<2149::aid-hyp847>3.0.co;2-8, 1999. 4251

Boe, J., Terray, L., Habets, F., and Martin, E.: Statistical and dynamical downscaling of the Seine basin climate for hydro-meteorological studies, *Int. J. Climatol.*, 27, 1643–1655, doi:10.1002/joc.1602, 2007. 4249

Bogner, K., Pappenberger, F., and Cloke, H. L.: Technical Note: The normal quantile transformation and its application in a flood forecasting system, *Hydrol. Earth Syst. Sci.*, 16, 1085–1094, doi:10.5194/hess-16-1085-2012, 2012. 4250

Cayan, D. R., Riddle, L. G., and Aguado, E.: The influence of precipitation and temperature on seasonal streamflow in California, *Water Resour. Res.*, 29, 1127–1140, doi:10.1029/92wr02802, 1993. 4243, 4262

Clark, M. P. and Hay, L. E.: Use of medium-range numerical weather prediction model output to produce forecasts of streamflow, *J. Hydrometeorol.*, 5, 15–32, doi:10.1175/1525-7541(2004)005<0015:uomnwp>2.0.co;2, 2004. 4243

Clark, M. P., Slater, A. G., Barrett, A. P., Hay, L. E., McCabe, G. J., Rajagopalan, B., and Leavesley, G. H.: Assimilation of snow covered area information into hydrologic and land-surface models, *Adv. Water. Resour.*, 29, 1209–1221, doi:10.1016/j.advwatres.2005.10.001, 2006. 4244

Day, G. N.: Extended streamflow forecasting using NWSRFS, *J. Water Res. Pl.-ASCE*, 111, 157–170, 1985. 4243

Dutra, E., Kotlarski, S., Viterbo, P., Balsamo, G., Miranda, P. M. A., Schär, C., Bissolli, P., and Jonas, T.: Snow cover sensitivity to horizontal resolution, parameterizations, and atmospheric forcing in a land surface model, *J. Geophys. Res.-Atmos.*, 116, D21109, doi:10.1029/2011jd016061, 2011. 4243

FOEN: Hydrological Atlas of Switzerland [electronical data], Federal Office for the Environment, 2010. 4243, 4244

Foppa, N. and Seiz, G.: Inter-annual variations of snow days over Switzerland from 2000–2010 derived from MODIS satellite data, *The Cryosphere*, 6, 331–342, doi:10.5194/tc-6-331-2012, 2012. 4243

- Foppa, N., Stoffel, A., and Meister, R.: Snow depth mapping in the Alps: merging of in situ and remotely-sensed data., *EARSel eProceedings*, 4, 119–129, 2005. 4243, 4244
- Foppa, N., Stoffel, A., and Meister, R.: Synergy of in situ and space borne observation for snow depth mapping in the Swiss Alps, *Int. J. Appl. Earth Obs.*, 9, 294–310, doi:10.1016/j.jag.2006.10.001, 2007. 4244, 4250
- Fundel, F., Walser, A., Liniger, M. A., Frei, C., and Appenzeller, C.: Calibrated precipitation forecasts for a limited-area ensemble forecast system using reforecasts, *Mon. Weather Rev.*, 138, 176–189, doi:10.1175/2009mwr2977.1, 2010. 4249
- Fundel, F., Jörg-Hess, S., and Zappa, M.: Monthly hydrometeorological ensemble prediction of streamflow droughts and corresponding drought indices, *Hydrol. Earth Syst. Sci.*, 17, 395–407, doi:10.5194/hess-17-395-2013, 2013. 4263
- Gurtz, J., Baltensweiler, A., and Lang, H.: Spatially distributed hydrotope-based modelling of evapotranspiration and runoff in mountainous basins, *Hydrol. Process.*, 13, 2751–2768, doi:10.1002/(SICI)1099-1085(19991215)13:17<2751::AID-HYP897>3.3.CO;2-F, 1999. 4257
- Hamill, T. M. and Whitaker, J. S.: Probabilistic quantitative precipitation forecasts based on reforecast analogs: theory and application, *Mon. Weather Rev.*, 134, 3209–3229, 2006. 4250
- Hock, R., Rees, G., Williams, M. W., and Ramirez, E.: Preface – contribution from glaciers and snow cover to runoff from mountains in different climates – special issue, *Hydrol. Process.*, 20, 2089–2090, doi:10.1002/hyp.6206, 2006. 4243
- Ines, A. V. M. and Hansen, J. W.: Bias correction of daily GCM rainfall for crop simulation studies, *Agr. Forest. Meteorol.*, 138, 44–53, doi:10.1016/j.agrformet.2006.03.009, 2006. 4249
- Jonas, T., Marty, C., and Magnusson, J.: Estimating the snow water equivalent from snow depth measurements in the Swiss Alps, *J. Hydrol.*, 378, 161–167, doi:10.1016/j.jhydrol.2009.09.021, 2009. 4244, 4248, 4250
- Kobierska, F., Jonas, T., Zappa, M., Bavay, M., Magnusson, J., and Bernasconi, S. M.: Future runoff from a partly glacierized watershed in Central Switzerland: a two-model approach, *Adv. Water Resour.*, 55, 204–214, doi:10.1016/j.apgeochem.2011.03.029, 2013. 4257
- Koster, R. D., Mahanama, S. P. P., Livneh, B., Lettenmaier, D. P., and Reichle, R. H.: Skill in streamflow forecasts derived from large-scale estimates of soil moisture and snow, *Nat. Geosci.*, 3, 613–616, doi:10.1038/ngeo944, 2010. 4243
- Latnser, M. and Schneebeli, M.: Long-term snow climate trends of the Swiss Alps (1931–1999), *Int. J. Climatol.*, 23, 733–750, doi:10.1002/joc.912, 2003. 4243

## Refining SWE climatologies in Alpine terrain

S. Jörg-Hess et al.

Title Page

Abstract

Introduction

Conclusions

References

Tables

Figures

◀

▶

◀

▶

Back

Close

Full Screen / Esc

Printer-friendly Version

Interactive Discussion



## Refining SWE climatologies in Alpine terrain

S. Jörg-Hess et al.

Title Page

Abstract

Introduction

Conclusions

References

Tables

Figures

◀

▶

◀

▶

Back

Close

Full Screen / Esc

Printer-friendly Version

Interactive Discussion



- Li, H. B., Sheffield, J., and Wood, E. F.: Bias correction of monthly precipitation and temperature fields from Intergovernmental Panel on Climate Change AR4 models using equidistant quantile matching, *J. Geophys. Res.-Atmos.*, 115, D10101, doi:10.1029/2009jd012882, 2010. 4249, 4250, 4261
- 5 Mauser, W., Prasch, M., and Strasser, U.: Physically based modelling of climate change impact on snow cover dynamics in Alpine regions using a stochastic weather generator, *Modsim 2007: International Congress on Modelling and Simulation: Land, Water and Environmental Management: Integrated Systems for Sustainability*, 2007. 4243
- Pagano, T. C., Garen, D. C., Perkins, T. R., and Pasteris, P. A.: Daily updating of operational statistical seasonal water supply forecasts for the western US1, *JAWRA J. Am. Water Resour. As.*, 45, 767–778, doi:10.1111/j.1752-1688.2009.00321.x, 2009. 4243
- 10 Panofsky, H. A. and Brier, G. W.: Some applications of statistics to meteorology, in: *Earth and Mineral Sciences Continuing Education College of Earth and Mineral Sciences, The Pennsylvania State University, University Park, Pennsylvania*, 1968. 4245, 4249
- 15 Parajka, J. and Blöschl, G.: The value of MODIS snow cover data in validating and calibrating conceptual hydrologic models, *J. Hydrol.*, 358, 240–258, doi:10.1016/j.jhydrol.2008.06.006, 2008. 4243
- Poulin, A., Brissette, F., Leconte, R., Arsenault, R., and Malo, J. S.: Uncertainty of hydrological modelling in climate change impact studies in a Canadian, snow-dominated river basin, *J. Hydrol.*, 409, 626–636, doi:10.1016/j.jhydrol.2011.08.057, 2011. 4243
- 20 Saloranta, T. M.: Simulating snow maps for Norway: description and statistical evaluation of the seNorge snow model, *The Cryosphere*, 6, 1323–1337, doi:10.5194/tc-6-1323-2012, 2012. 4250
- Schär, C., Vasilina, L., Pertziger, F., and Dirren, S.: Seasonal runoff forecasting using precipitation from meteorological data assimilation systems, *J. Hydrometeorol.*, 5, 959–973, doi:10.1175/1525-7541(2004)005<0959:srfupf>2.0.co;2, 2004. 4243
- 25 Sevruk, B.: Correction of Precipitation Measurements, *ETH/IASH/WMO Workshop on the Correction of Precipitation Measurements*, vol. 23, ETH Zürich, 1986. 4243
- Slater, A. G. and Clark, M. P.: Snow data assimilation via an ensemble Kalman filter, *J. Hydrometeorol.*, 7, 478–493, doi:10.1175/JHM505.1, 2006. 4244
- 30 Steger, C., Kotlarski, S., Jonas, T., and Schär, C.: Alpine snow cover in a changing climate: a regional climate model perspective, *Clim. Dynam.*, 1–20, doi:10.1007/s00382-012-1545-3, 2012. 4243

**Refining SWE climatologies in Alpine terrain**

S. Jörg-Hess et al.

Title Page

Abstract

Introduction

Conclusions

References

Tables

Figures

◀

▶

◀

▶

Back

Close

Full Screen / Esc

Printer-friendly Version

Interactive Discussion

Sturm, M., Taras, B., Liston, G. E., Derksen, C., Jonas, T., and Lea, J.: Estimating snow water equivalent using snow depth data and climate classes, *J. Hydrometeorol.*, 11, 1380–1394, doi:10.1175/2010jhm1202.1, 2010. 4244, 4246, 4260

Thayyen, R. J. and Gergan, J. T.: Role of glaciers in watershed hydrology: a preliminary study of a “Himalayan catchment”, *The Cryosphere*, 4, 115–128, doi:10.5194/tc-4-115-2010, 2010. 4243

Themeßl, M. J., Gobiet, A., and Leuprecht, A.: Empirical-statistical downscaling and error correction of daily precipitation from regional climate models, *Int. J. Climatol.*, 31, 1530–1544, doi:10.1002/joc.2168, 2011. 4249, 4250

Thrasher, B., Maurer, E. P., McKellar, C., and Duffy, P. B.: Technical Note: Bias correcting climate model simulated daily temperature extremes with quantile mapping, *Hydrol. Earth Syst. Sci.*, 16, 3309–3314, doi:10.5194/hess-16-3309-2012, 2012. 4249

Veijalainen, N., Korhonen, J., Vehviläinen, B., and Koivusalo, H.: Modelling and statistical analysis of catchment water balance and discharge in Finland in 1951–2009 using transient climate scenarios, *J. Water Climate Change*, 3, 55–78, doi:10.2166/wcc.2012.012, 2012. 4249

Viviroli, D., Weingartner, R., and Messerli, B.: Assessing the hydrological significance of the world’s mountains, *Mt. Res. Dev.*, 23, 32–40, doi:10.1659/0276-4741(2003)023[0032:athstot]2.0.co;2, 2003. 4243

Viviroli, D., Gurtz, J., and Zappa, M.: The Hydrological Modelling System Part II: Physical Model Description, *Geographica Bernensia P40*, Institute of Geography, University of Berne, Bern, 2007. 4257

Viviroli, D., Mittelbach, H., Gurtz, J., and Weingartner, R.: Continuous simulation for flood estimation in ungauged mesoscale catchments of Switzerland – Part II: Parameter regionalisation and flood estimation results, *J. Hydrol.*, 377, 208–225, doi:10.1016/j.jhydrol.2009.08.022, 2009a. 4257

Viviroli, D., Zappa, M., Schwanbeck, J., Gurtz, J., and Weingartner, R.: Continuous simulation for flood estimation in ungauged mesoscale catchments of Switzerland – Part I: Modelling framework and calibration results, *J. Hydrol.*, 377, 191–207, doi:10.1016/j.jhydrol.2009.08.023, 2009b. 4257

Weisberg, S.: *Applied Linear Regression*, 3rd edn., Wiley-Interscience, Hoboken, NJ, 2005. 4259

- Wilks, D. S.: Statistical Methods in the Atmospheric Sciences, International Geophysics Series, 2nd edn., Academic Press, Amsterdam, Boston, 2006. 4250
- Witmer, U., Filliger, P., Kunz, S., and Küng, P.: Recording, Processing And Mapping of Snow Data in Switzerland, Geographica Bernensia G25, University of Bern, Switzerland, 1986. 4244
- 5 Wood, A. W., Leung, L. R., Sridhar, V., and Lettenmaier, D. P.: Hydrologic implications of dynamical and statistical approaches to downscaling climate model outputs, Climatic Change, 62, 189–216, doi:10.1023/B:CLIM.0000013685.99609.9e, 2004. 4249
- 10 Zappa, M., Pos, F., Strasser, U., Warmerdam, P., and Gurtz, J.: Seasonal water balance of an Alpine catchment as evaluated by different methods for spatially distributed snowmelt modelling, Nord Hydrol., 34, 179–202, 2003. 4257
- Zappa, M., Bernhard, L., Fundel, F., and Jörg-Hess, S.: Forecasts and Scenarios of Snow and Water Resources in Alpine Environments, Forum für Wissen, 19–27, 2012 (in German). 4246

## Refining SWE climatologies in Alpine terrain

S. Jörg-Hess et al.

[Title Page](#)[Abstract](#)[Introduction](#)[Conclusions](#)[References](#)[Tables](#)[Figures](#)[◀](#)[▶](#)[◀](#)[▶](#)[Back](#)[Close](#)[Full Screen / Esc](#)[Printer-friendly Version](#)[Interactive Discussion](#)

## Refining SWE climatologies in Alpine terrain

S. Jörg-Hess et al.

**Table 1.** Characteristics of the three regions Alpenrhein (AR), Valais (VS) and Thur/Toess/Glatt (TTG).

	AR	TTG	VS
Size [km <sup>2</sup> ]	6342	2586	5382
Mean elevation [m a.s.l.]	1742	696	2078
Min elevation [m a.s.l.]	409	345	372
Max elevation [m a.s.l.]	3361	2324	4403
% above 2000	39	0.4	56

[Title Page](#)
[Abstract](#)
[Introduction](#)
[Conclusions](#)
[References](#)
[Tables](#)
[Figures](#)
[Back](#)
[Close](#)
[Full Screen / Esc](#)
[Printer-friendly Version](#)
[Interactive Discussion](#)


## Refining SWE climatologies in Alpine terrain

S. Jörg-Hess et al.

**Table 2.** Statistical scores of *map110* and *map.cal* for the three catchments AR, TTG and VS. Stars mark significant differences between *map110* and *map.cal* (at a 95 % confidence level).

	AR		TTG		VS	
	map110	map.cal	map110	map.cal	map110	map.cal
ME	-18.21	0.01*	-4.33	0.47	-22.89	-0.76*
$R^2$	0.86	0.81*	0.84	0.79*	0.75	0.7*
RMSE	53.88	48.32*	13.91	9.26*	78.43	60.78*

[Title Page](#)
[Abstract](#)
[Introduction](#)
[Conclusions](#)
[References](#)
[Tables](#)
[Figures](#)
[Back](#)
[Close](#)
[Full Screen / Esc](#)
[Printer-friendly Version](#)
[Interactive Discussion](#)


## TCD

7, 4241–4286, 2013

## Refining SWE climatologies in Alpine terrain

S. Jörg-Hess et al.

Title Page

Abstract

Introduction

Conclusions

References

Tables

Figures

◀

▶

◀

▶

Back

Close

Full Screen / Esc

Printer-friendly Version

Interactive Discussion



**Table 3.** RMSEs [mm] at the stations AN, BI, OB and PA. *Map203* and *map.cal* are the original versions. *Map203<sup>-</sup>* and *map.cal<sup>-</sup>* are the maps with the four stations removed.

	<i>map203</i>	<i>map203<sup>-</sup></i>	<i>map.cal</i>	<i>map.cal<sup>-</sup></i>
AN	56	72	101	108
BN	101	140	96	132
OB	33	39	37	40
PA	20	30	63	59

- 1971 – 2009 (d110)
- 1989 – 2009 (d133)
- 2001 – 2009 (d203)

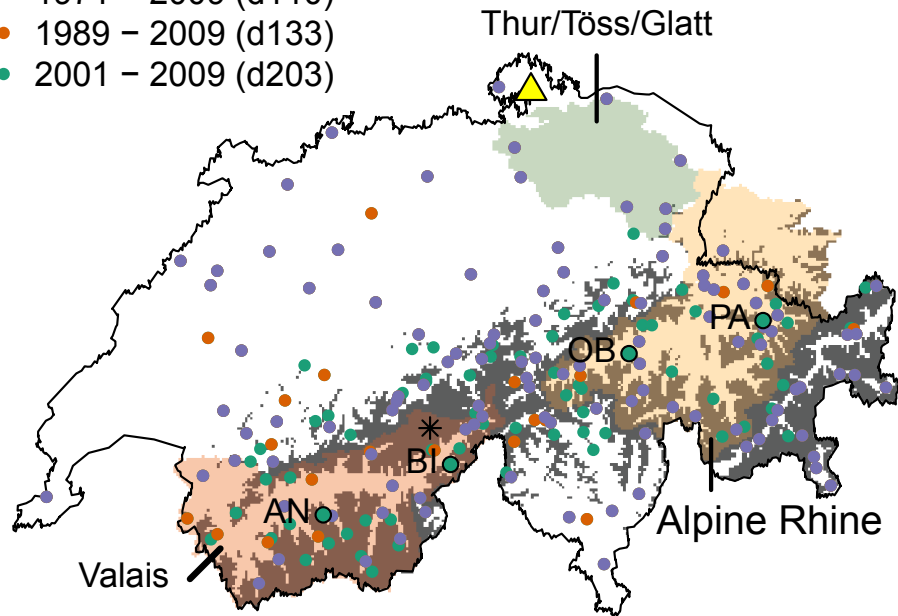


**Fig. 1.** Stations available during the different time periods: 110 stations from 1971–2009 (purple dots), 133 stations from 1989–2009 (purple and orange dots) and 203 stations from 2001–2009 (purple, orange and green dots). The three sub-areas, Alpine Rhein (AR), Valais (VS) and the region including the rivers Thur, Toess and Glatt (TTG) are considered in this study. Areas shaded grey are higher than 2000 m a.s.l. The four labeled stations with black outlines are used for validation. The yellow triangle is the river gauge in Neuhausen. The black star is a randomly chosen grid cell for the example in Sect. 4.3.

**Refining SWE climatologies in Alpine terrain**

S. Jörg-Hess et al.

Title Page	
Abstract	Introduction
Conclusions	References
Tables	Figures
◀	▶
◀	▶
Back	Close
Full Screen / Esc	
Printer-friendly Version	
Interactive Discussion	



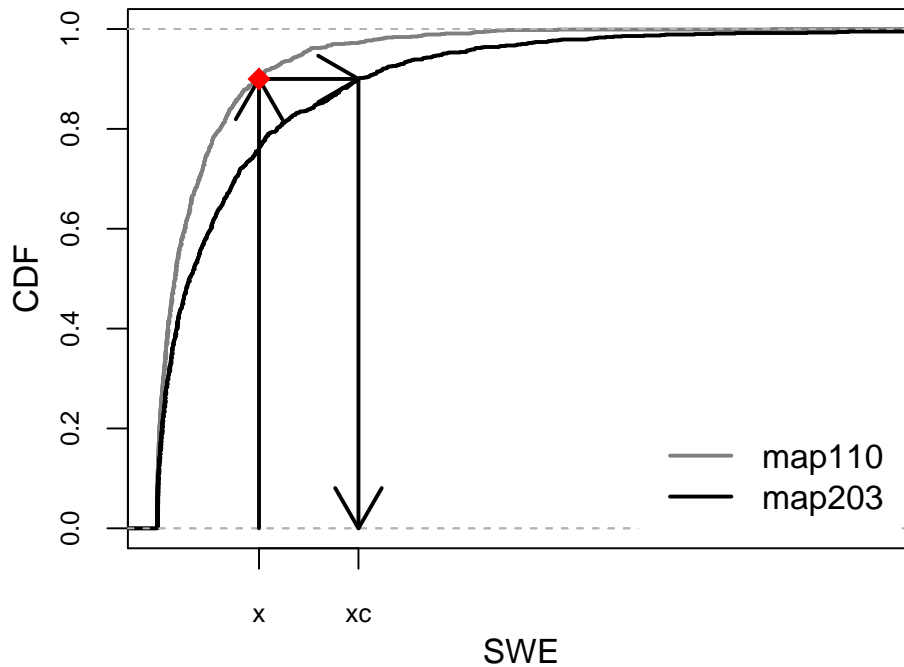


**Fig. 2.** Illustration of quantile mapping.  $X$  is the value to calibrate. The red diamond corresponds to the non-exceedance probability of  $x$  with respect to *map110*.  $X_c$  is the calibrated value, which is the value of the same non-exceedance probability with respect to *map203*.

**Refining SWE climatologies in Alpine terrain**

S. Jörg-Hess et al.

Title Page	
Abstract	Introduction
Conclusions	References
Tables	Figures
⏪	⏩
◀	▶
Back	Close
Full Screen / Esc	
Printer-friendly Version	
Interactive Discussion	



Refining SWE climatologies in Alpine terrain

S. Jörg-Hess et al.

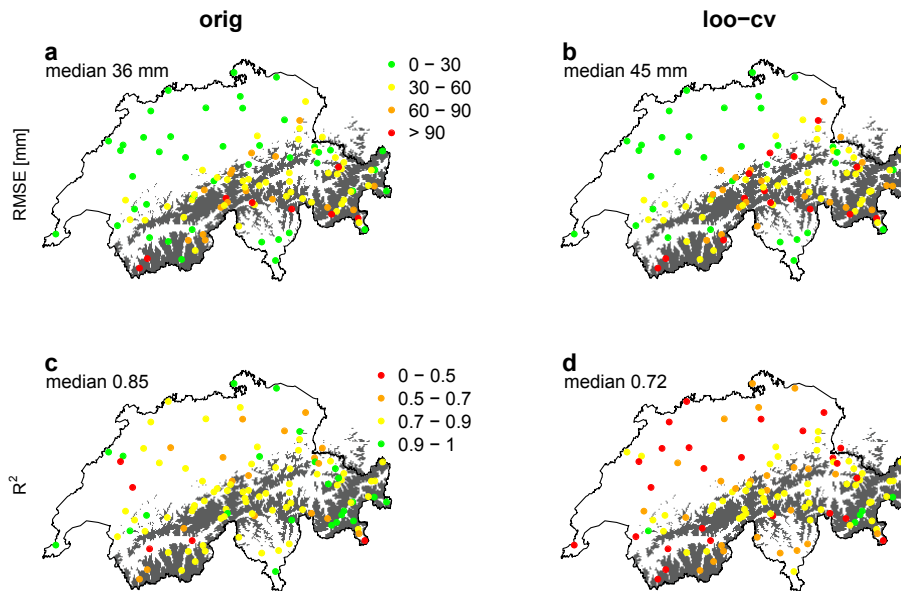


**Fig. 3.** Statistics for the SWE maps at station grid cells averaged over the period 2001–2009. The left column (**a** and **c**) contains the scores calculated with  $SWE_{orig}$  and the right (**b** and **d**) those based on  $SWE_{loo-cv}$ . Areas shaded grey are higher than 2000 m a.s.l.

Title Page

Abstract Introduction

Conclusions References

Tables Figures

◀ ▶

◀ ▶

Back Close

Full Screen / Esc

Printer-friendly Version

Interactive Discussion



Refining SWE climatologies in Alpine terrain

S. Jörg-Hess et al.

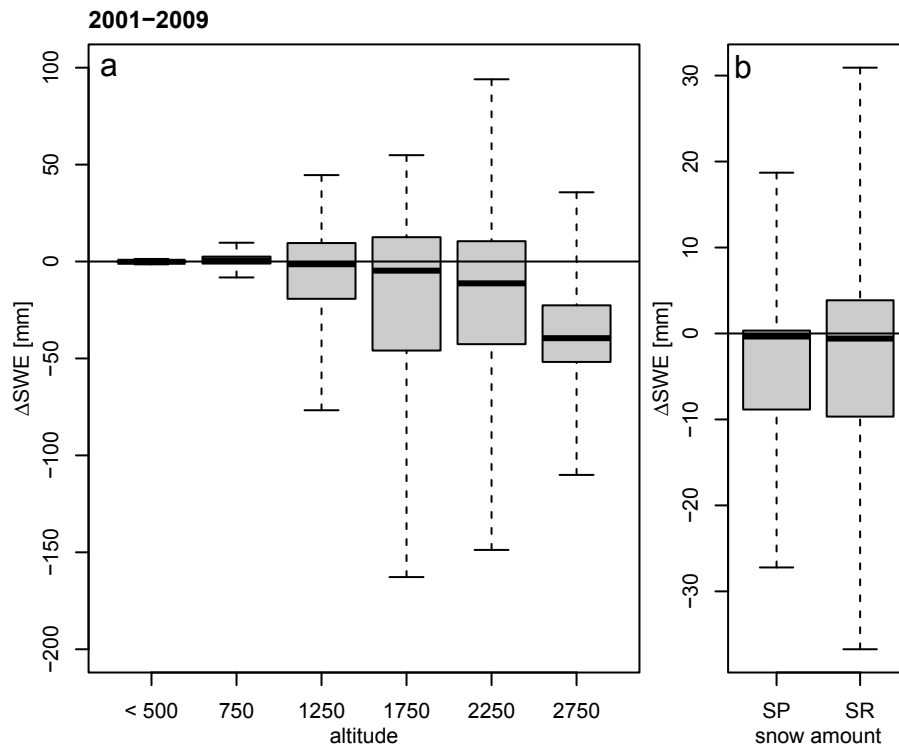


**Fig. 4.** The mean differences between *map110*–*map203* per grid cell for: **(a)** different altitude ranges and **(b)** snow-rich and snow-poor days in the whole of Switzerland during the overlapping period (2001–2009). The boxes display the median and the interquartile range (IQR). The whiskers extend to the maximum  $\Delta SWE$ , but are limited by twice of the interquartile range.

Title Page

Abstract Introduction

Conclusions References

Tables Figures

◀ ▶

◀ ▶

Back Close

Full Screen / Esc

Printer-friendly Version

Interactive Discussion



## Refining SWE climatologies in Alpine terrain

S. Jörg-Hess et al.

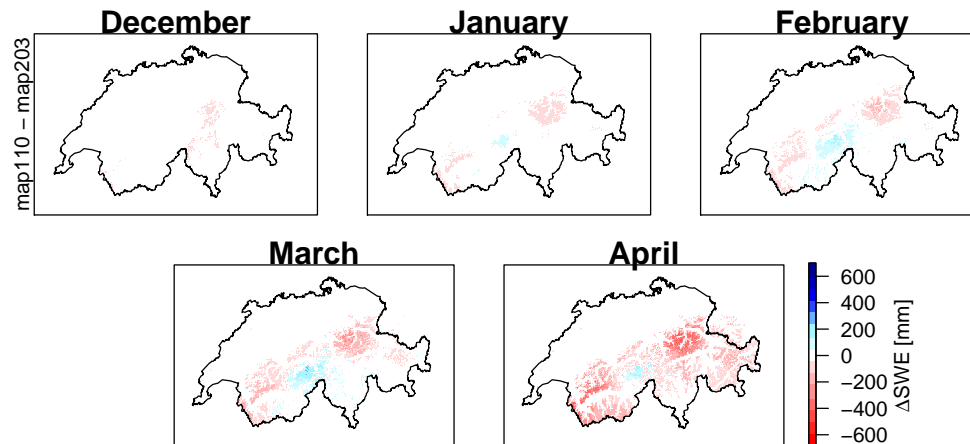


**Fig. 5.** The mean differences ( $map110 - map203$ ) per grid cell for the five winter months December, January, February, March and April (2001–2009).

[Title Page](#)[Abstract](#)[Introduction](#)[Conclusions](#)[References](#)[Tables](#)[Figures](#)[◀](#)[▶](#)[◀](#)[▶](#)[Back](#)[Close](#)[Full Screen / Esc](#)[Printer-friendly Version](#)[Interactive Discussion](#)

## Refining SWE climatologies in Alpine terrain

S. Jörg-Hess et al.

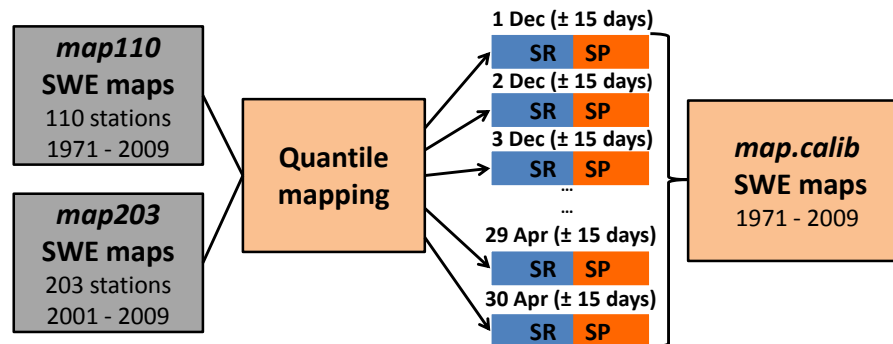


**Fig. 6.** Calibration procedure. SR refers to snow-rich and SP to snow-poor days. The distinction between SR and SP is based on the median of *map110* during the overlapping period.

Title Page

Abstract

Introduction

Conclusions

References

Tables

Figures

◀

▶

◀

▶

Back

Close

Full Screen / Esc

Printer-friendly Version

Interactive Discussion



## Refining SWE climatologies in Alpine terrain

S. Jörg-Hess et al.

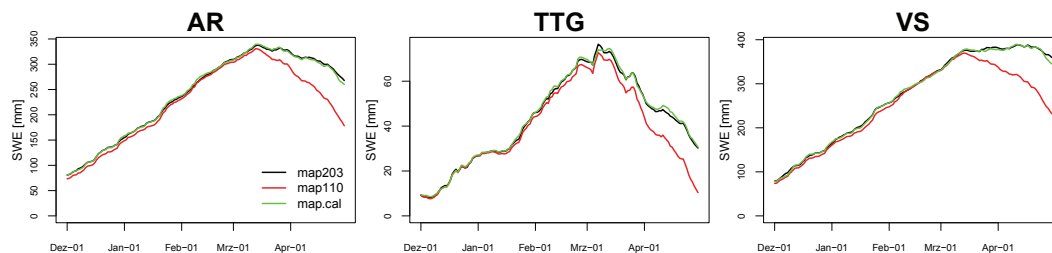


**Fig. 7.** Daily mean SWE averaged over the catchment and the nine years of the calibration period: Alpine Rhine (AR), Thur/Toess/Glatt (TTG) and Valais (VS).

[Title Page](#)[Abstract](#)[Introduction](#)[Conclusions](#)[References](#)[Tables](#)[Figures](#)[◀](#)[▶](#)[◀](#)[▶](#)[Back](#)[Close](#)[Full Screen / Esc](#)[Printer-friendly Version](#)[Interactive Discussion](#)

## Refining SWE climatologies in Alpine terrain

S. Jörg-Hess et al.

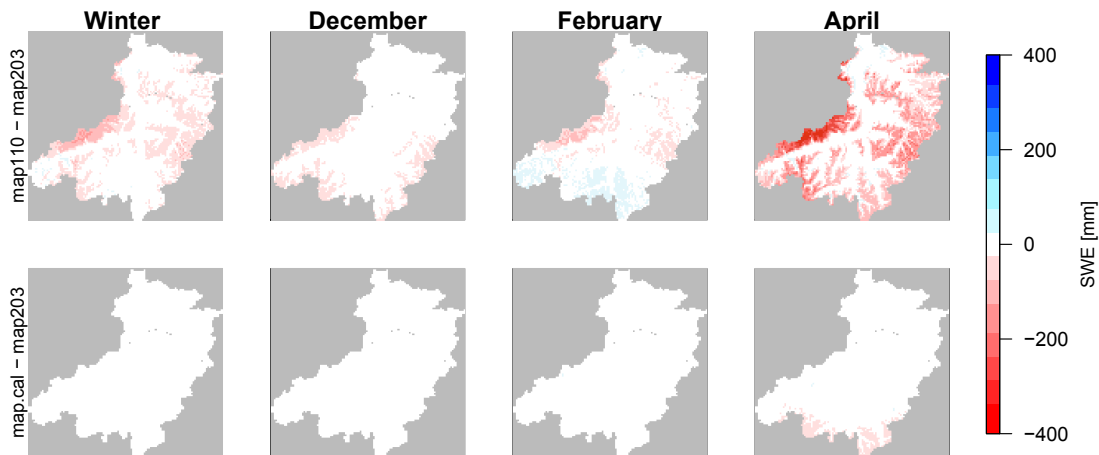


**Fig. 8.** Mean differences between *map110*–*map203* (top) and *map.cal*–*map203* (bottom) for the whole winter, and for December, February, and April (2001–2009) for the AR region.

[Title Page](#)[Abstract](#)[Introduction](#)[Conclusions](#)[References](#)[Tables](#)[Figures](#)[⏪](#)[⏩](#)[◀](#)[▶](#)[Back](#)[Close](#)[Full Screen / Esc](#)[Printer-friendly Version](#)[Interactive Discussion](#)

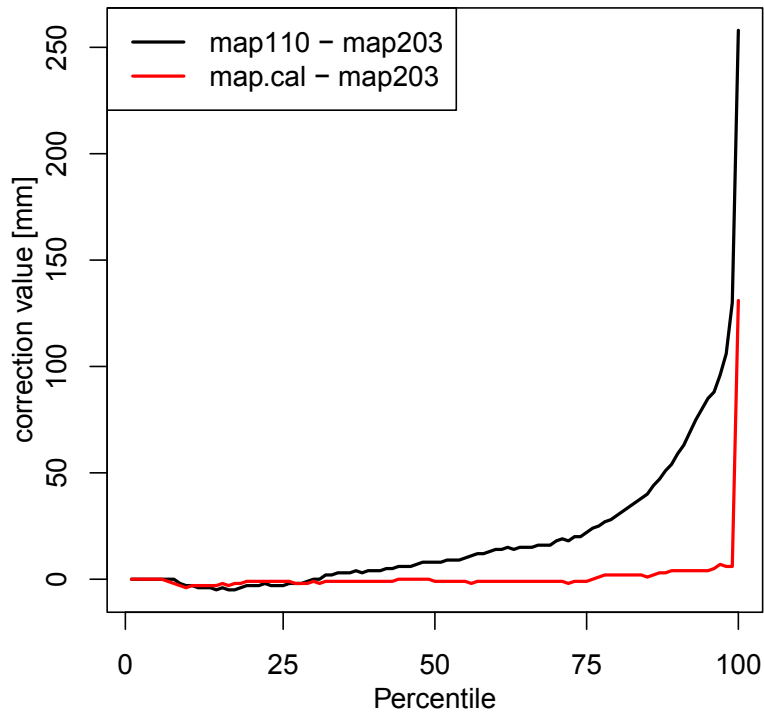


**Fig. 9.** Differences in percentiles between *map203* and *map110* (black line) and *map203* and *map.cal* (red line) for the Alpine Rhine during the calibration period.

**Refining SWE climatologies in Alpine terrain**

S. Jörg-Hess et al.

Title Page

Abstract Introduction

Conclusions References

Tables Figures

◀ ▶

◀ ▶

Back Close

Full Screen / Esc

Printer-friendly Version

Interactive Discussion



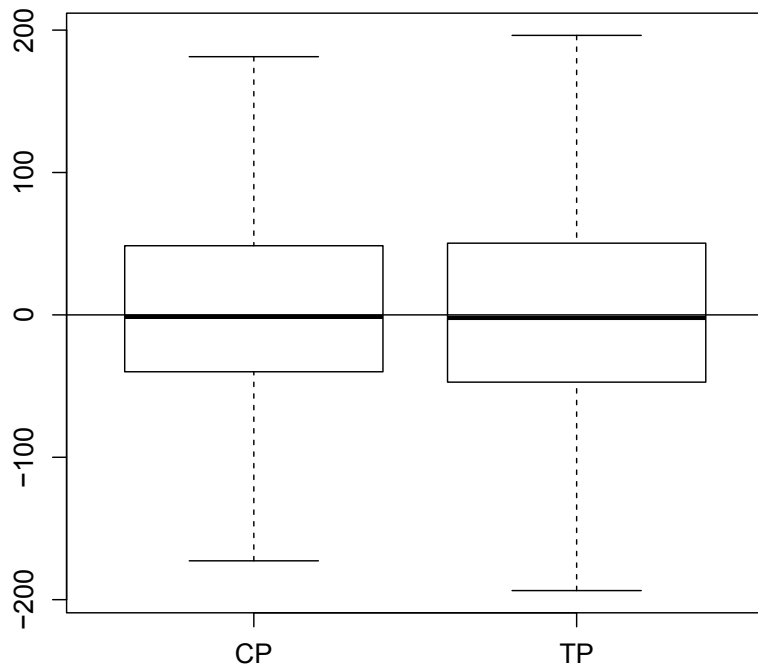


**Fig. 10.** Mean differences in the calibrated and observed SWE at 23 stations for the calibration period (left) and the test period (right). Box and whiskers are shown as in Fig. 4.

**Refining SWE climatologies in Alpine terrain**

S. Jörg-Hess et al.

Title Page

Abstract Introduction

Conclusions References

Tables Figures

◀ ▶

◀ ▶

Back Close

Full Screen / Esc

Printer-friendly Version

Interactive Discussion



## Refining SWE climatologies in Alpine terrain

S. Jörg-Hess et al.

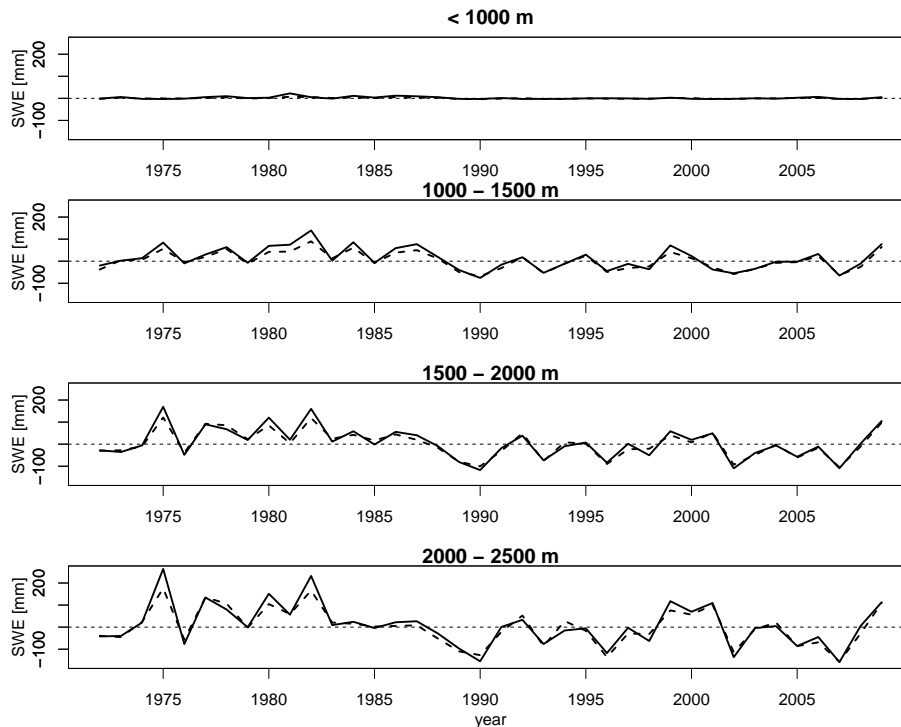


**Fig. 11.** Anomalies in the median winter SWE [mm] in *map110* (black line) and *map.cal* (dashed line) for different altitude classes.

Title Page

Abstract

Introduction

Conclusions

References

Tables

Figures

◀

▶

◀

▶

Back

Close

Full Screen / Esc

Printer-friendly Version

Interactive Discussion



Refining SWE climatologies in Alpine terrain

S. Jörg-Hess et al.

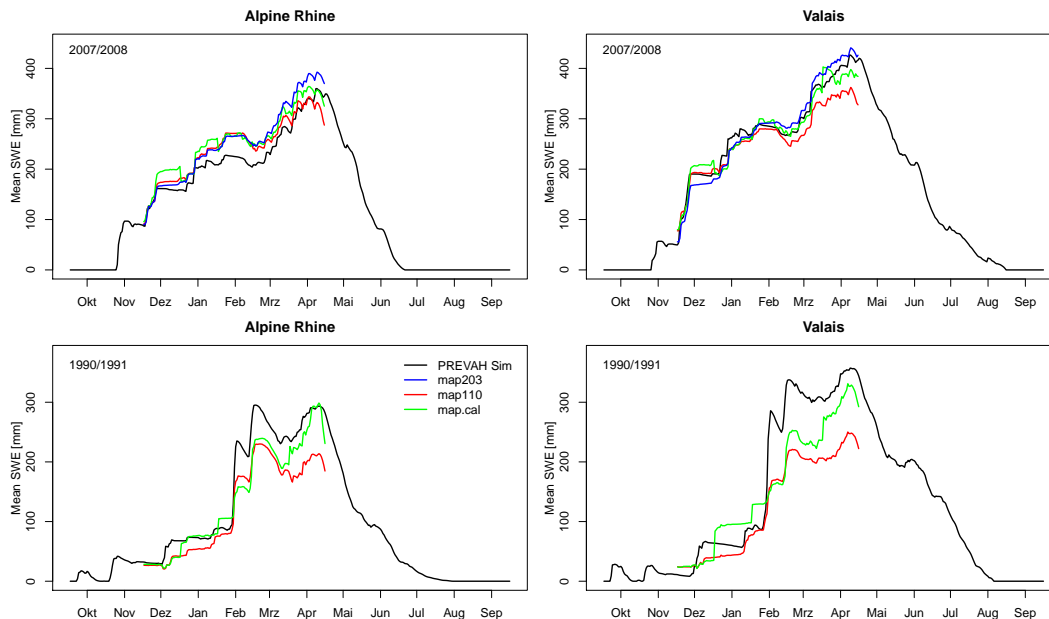


**Fig. 12.** Daily mean SWE in the Alpine Rhine catchment (left) and the Valais (right) for the hydrological years 2008 (top) and 1991 (bottom). SWE is illustrated as PREVAH simulations (black), *map203* (blue), *map110* (red) and *map110 cal* (green).

Title Page

Abstract Introduction

Conclusions References

Tables Figures

◀ ▶

◀ ▶

Back Close

Full Screen / Esc

Printer-friendly Version

Interactive Discussion



## Refining SWE climatologies in Alpine terrain

S. Jörg-Hess et al.

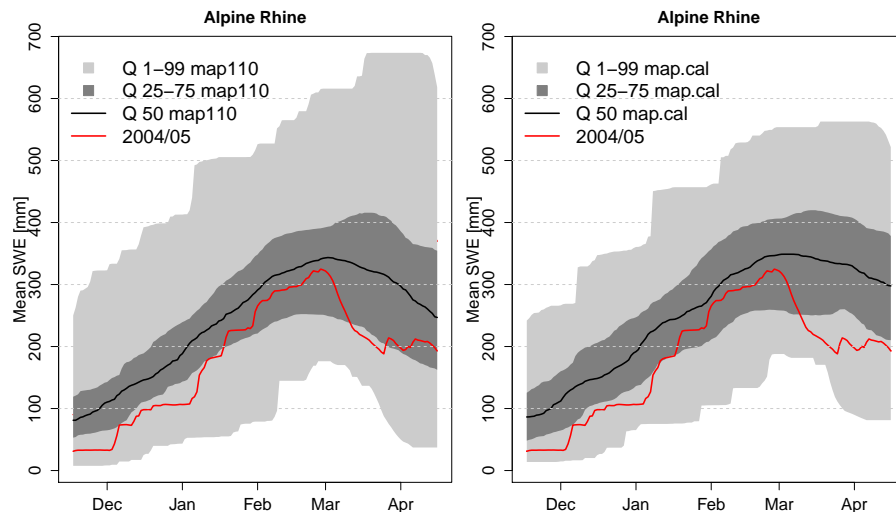


**Fig. 13.** SWE range and interquartile range for the period 1971–2009 in the Alpine Rhine catchment from *map110* (left) and *map.cal* (right). The climatologies are calculated for daily mean SWE with a window of  $\pm 10$  days around the day of interest. The red line is SWE for the year 2004/2005, based on *map203*.

Title Page

Abstract

Introduction

Conclusions

References

Tables

Figures

◀

▶

◀

▶

Back

Close

Full Screen / Esc

Printer-friendly Version

Interactive Discussion



## Refining SWE climatologies in Alpine terrain

S. Jörg-Hess et al.

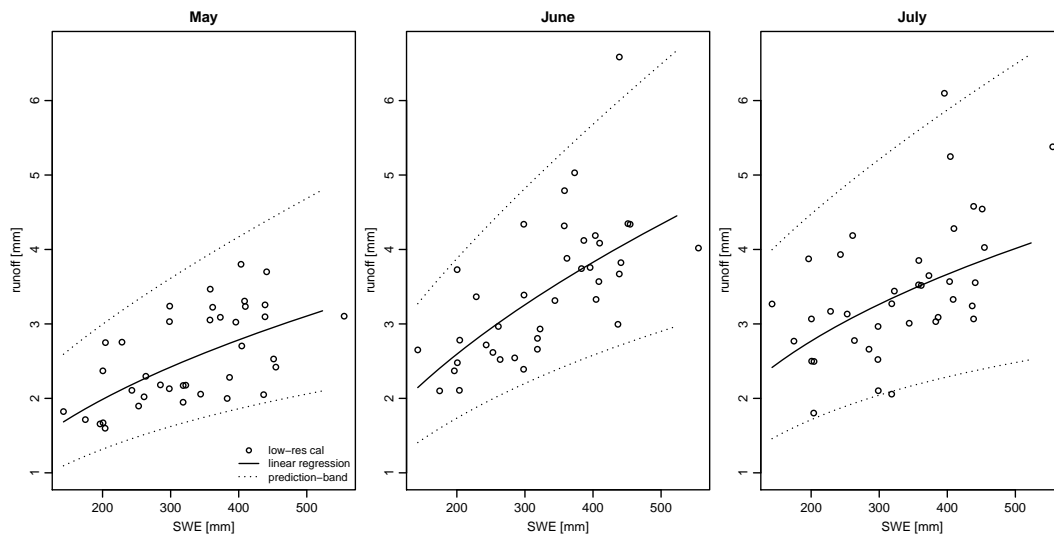


**Fig. 14.** The minimum runoff in May (left), June (middle) and July (right) explained by the SWE on 15 April through linear regression. SWE (black circles) are based on *map.cal*. The black line is the linear regression line. The dotted line marks the prediction band.

Title Page

Abstract

Introduction

Conclusions

References

Tables

Figures

◀

▶

◀

▶

Back

Close

Full Screen / Esc

Printer-friendly Version

Interactive Discussion



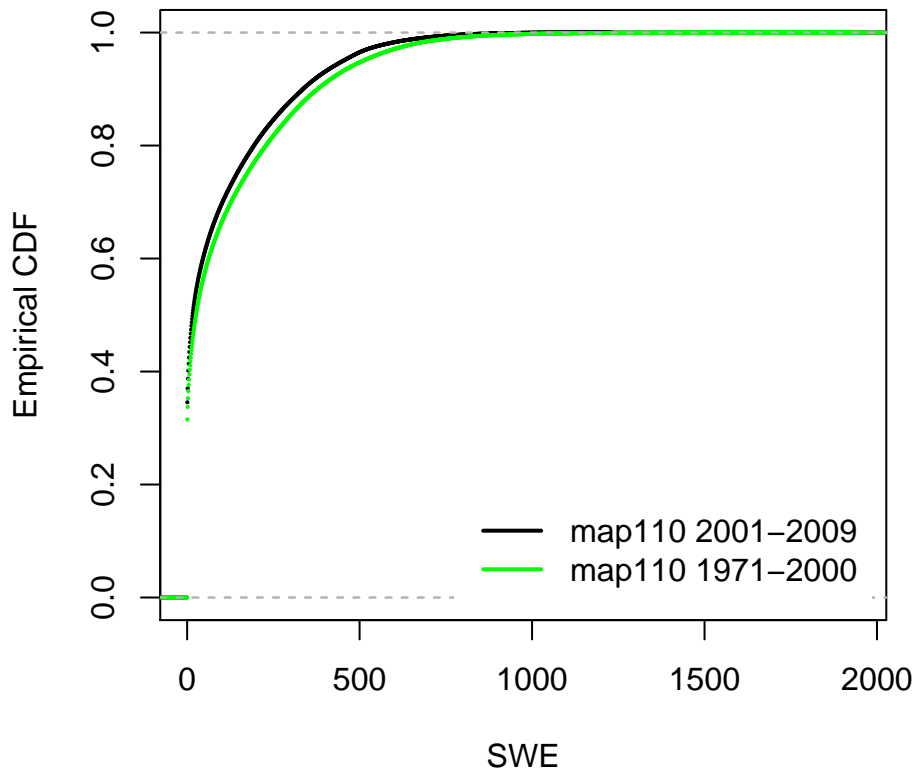


**Fig. 15.** Comparison of the SWE distribution in *map110* during the training period (black) and the calibration period (green).

**Refining SWE climatologies in Alpine terrain**

S. Jörg-Hess et al.

Title Page

Abstract Introduction

Conclusions References

Tables Figures

◀ ▶

◀ ▶

Back Close

Full Screen / Esc

Printer-friendly Version

Interactive Discussion

